frontiers in Marine Science

ORIGINAL RESEARCH
published: 21 June 2021
doi: 10.3389/fmars.2021.683354

Diatom Dominance Enhances Resistance of Phytoplanktonic POM to Mesopelagic Microbial Decomposition

Miguel Cabrera-Brufau[1,2], Laura Arin[1], Maria Montserrat Sala[1], Pedro Cermeño[1†] and Cèlia Marrasé[1†]*

[1] *Departamento de Biología Marina y Oceanografía, Instituto de Ciencias del Mar, Consejo Superior de Investigaciones Científicas, Barcelona, Spain,* [2] *Departamento de Biología Evolutiva, Ecología y Ciencias Ambientales, Universidad de Barcelona, Barcelona, Spain*

OPEN ACCESS

Edited by:
Marius Nils Müller, Federal University of Pernambuco, Brazil

Reviewed by:
Haimanti Biswas, National Institute of Oceanography, Council of Scientific and Industrial Research (CSIR), India
Frederico Pereira Brandini, University of São Paulo, Brazil

****Correspondence:***
Miguel Cabrera-Brufau
cabrera@icm.csic.es

† These authors have contributed equally to this work and share last authorship

Specialty section:
This article was submitted to Marine Biogeochemistry, a section of the journal Frontiers in Marine Science

Received: *20 March 2021*
Accepted: *28 May 2021*
Published: *21 June 2021*

Citation:
Cabrera-Brufau M, Arin L, Sala MM, Cermeño P and Marrasé C (2021) Diatom Dominance Enhances Resistance of Phytoplanktonic POM to Mesopelagic Microbial Decomposition. Front. Mar. Sci. 8:683354. doi: 10.3389/fmars.2021.683354

Particulate organic matter (POM) lability is one of the key factors determining the residence time of organic carbon (OC) in the marine system. Phytoplankton community composition can influence the rate at which heterotrophic microorganisms decompose phytoplankton detrital particles and thus, it controls the fraction of OC that reaches the ocean depths, where it can be sequestered for climate-relevant spans of time. Here, we compared the degradation dynamics of POM from phytoplankton assemblages of contrasting diatom dominance in the presence of mesopelagic prokaryotic communities during a 19-day degradation experiment. We found that diatom-derived POM exhibited an exponential decay rate approximately three times lower than that derived from a community dominated by flagellated phytoplankton (mainly coccolithophores and nanoflagellates). Additionally, dissolved organic matter (DOM) released during the degradation of diatom particles accumulated over the experiment, whereas only residual increases in DOM were detected during the degradation of non-diatom materials. These results suggest that diatom-dominance enhances the efficiencies of the biological carbon pump and microbial carbon pump through the relatively reduced labilities of diatom particles and of the dissolved materials that arise from their microbial processing.

Keywords: biodegradation experiment, marine phytoplankton, diatom, organic matter lability, particulate organic matter, dissolved organic matter, mesopelagic microbes

INTRODUCTION

Marine phytoplankton are responsible for approximately half of global net primary production (NPP), i.e., 53.6 ± 7.4 Pg C per year (Dunne et al., 2007) compared to a mean of 55 Pg C per year of terrestrial ecosystems (Cramer et al., 1999). Although most of the organic carbon (OC) produced in the euphotic layer of the ocean is consumed and remineralized *in situ*, approximately one fifth of NPP is exported out of the upper mixed layer, 3.4% of NPP is exported as dissolved organic matter (DOM) through overturning circulation (Hansell et al., 2009) and 17.9% of NPP as sinking particulate organic matter (POM) (Dunne et al., 2007; Carlson and Hansell, 2015).

This downward flux of organic matter (OM) constitutes the biological carbon pump (BCP) (Eppley and Peterson, 1979).

Exported POM flux is attenuated with depth resembling a power law function, the remineralization curve or Martin curve (Martin et al., 1987), and accounts for most (∼ 90%) of ocean respiration, with the remainder being supported by DOM (Aristegui et al., 2002). Prokaryotic decomposition activities are considered the main sink of marine POM in the mesopelagic ocean (200–1000 m depth), being responsible for up to 85–92% of particle remineralization by various estimates (Anderson and Tang, 2010; Giering et al., 2014). This implies the solubilization of sinking particles into DOM prior to prokaryotic uptake through zooplankton processing (Strom et al., 1997) and bacterial cleavage by extracellular enzymes (Smith et al., 1992). As such, the attenuation of POM flux with depth derives from the combined effects of particle remineralization into CO_2 and solubilization into DOM (Benner and Amon, 2015).

Two main climate relevant C-sequestration mechanisms arise from the downward export of OM. First, the classical BCP leads to part of the exported particulate organic carbon (POC) getting buried in marine sediments and, although this fraction is estimated to represent less than 1% of annual NPP (Carlson and Hansell, 2015), it represents one of the main biological mechanisms regulating atmospheric CO_2 at geological timescales (De La Rocha, 2007). Additionally, even if all NPP is remineralized before reaching the sediments, subtle differences in remineralization depth due to differences in the lability of organic materials, sinking velocities and/or deep convection of the exported POM can severely influence the storage and residence time of C in the dark ocean far from contact with the atmosphere (Kwon et al., 2009). The second mechanism consists in the accumulation of recalcitrant dissolved organic matter (RDOM) that arises from successive bacterial processing of readily available OM (Kramer and Herndl, 2004): the microbial carbon pump (MCP) (Jiao et al., 2010). The significance of the DOM pool is paramount, as it represents an enormous OC reservoir, comparable in magnitude to that of atmospheric CO_2 (Stone, 2010), of which 95% is RDOM, able to persist in the ocean with minimal losses for thousands of years (Hansell, 2013). The efficiencies of the BCP and MCP (i.e., the amount of C that is sequestered in the deep ocean by either of them relative to the NPP) depend, among other things, on (1) the set of processes that promote the downward export flux and (2) the degradability of the exported material. Phytoplankton community composition can alter both of these factors, and consequently has the potential of influencing the overall C-sequestration capacity of the oceans and thus Earth climate (Cermeño et al., 2008; Guidi et al., 2009; Siegel et al., 2014; Bach et al., 2019).

Phytoplankton cell size, shape, their ability to form colonies and the ballasting effect of mineral covers dictate sinking rates of individual groups (Padisák et al., 2003; Engel et al., 2009; Durante et al., 2019), modulating the overall export efficiency according to their dominance. Zooplankton activities can either diminish or increase export efficiencies and their net effect largely depends on the regionally variable plankton community structure (Steinberg and Landry, 2017). Heterotrophic prokaryotes lower C export by degrading and dissolving particles. However, they can also promote C export as they grow on non-sinking DOM, reintroducing this carbon to the trophic web and sinking POM fraction when they are grazed by larger consumers (del Giorgio and Cole, 1998). These trophic interactions have a profound impact in determining the export efficiency of a given system. Indeed, Guidi et al. (2009) found that 68% of the global variance in mass flux to 400 m depth could be explained by the phytoplankton community composition.

The mechanisms linking plankton community composition to particle degradability and remineralization in the meso- and bathypelagic oceans remain largely unknown (Herndl and Reinthaler, 2013). Particle C-specific remineralization rates are often modeled to be dependent on temperature alone (Schmittner et al., 2008; Bach et al., 2016) based on the fact that bacterial activity is largely dependent on this parameter (Pomeroy and Deibel, 1986). By contrast, the role of phytoplankton community composition in determining POM lability has long been overlooked. Its effects on particle size and porosity (Bach et al., 2019), the distinct macromolecular make-up of individual phylogenetic groups (Finkel et al., 2016) and their degree of cell wall mineralization (Engel et al., 2009; Moriceau et al., 2009) can influence the rate of particle degradation as they sink throughout the water column. This reflects how POM lability is not only dependent on seawater temperature and bacterial activity, but on the nature of the substrate and, consequently, on the identity of the phytoplankton that produced it.

Diatoms are dominant in many ecosystems; they are responsible for up to 35% of the total primary production in oligotrophic oceans and up to 75% in coastal waters and the Southern Ocean (Nelson et al., 1995; Tréguer et al., 1995). Jin et al. (2006) estimated their global contribution to NPP and to carbon export to be 15 and 40%, respectively. The ability of some diatoms to form resting spores, with highly silicified cell walls and enriched in lipids and carbohydrates (Kuwata et al., 1993), makes them very efficient at C-export. These cell forms appear to be extremely resistant to degradation and have the potential to dominate POC vertical fluxes to the deep ocean (Salter et al., 2012; Rembauville et al., 2016).

Experimental incubations, although not truly suitable to obtain specific values of POC attenuation, can be used to isolate and quantify the effects of different factors on carbon-specific remineralization rates, providing a more mechanistic approach and resulting in useful insights that can be used to improve model design and parametrization. The effects of temperature (Iversen and Ploug, 2013), mineral protection (Engel et al., 2009; Moriceau et al., 2009), and nutrient stress (Suroy et al., 2015) on POM remineralization rates have been examined in recent years. However, most studies use either natural POM of poorly constrained origin or monocultures that disregard the variable reactivity of natural POM. With the objective of studying the effect of phytoplankton community composition, with special emphasis on diatom contribution, on the degradation process of POM, we induced proliferations of contrasting diatom dominance from a natural marine plankton assemblage and followed their remineralization processes in the presence of mesopelagic prokaryotic communities for 19 days.

MATERIALS AND METHODS

Sampling

Seawater was collected 13.6 miles off Barcelona coast (41°15.80′ N, 2° 26.85′ E) during the AMICS field expedition on board the RV García del Cid (September 19, 2017). Two depths were sampled by means of rosette deployment: surface (5 m depth) and mesopelagic (200 m depth). The collected water was filtered on board; the surface volume was filtered through a 200-μm mesh to exclude large zooplankton, whereas the deeper one was filtered through 0.6 μm (ipPORE, 142 mm) to exclude any large particle. The filtered surface and mesopelagic waters were kept in a water bath during transit and then transferred to two temperature-controlled chambers at *in situ* temperatures (22 and 14°C, respectively).

Experimental Design

In order to investigate how the phytoplanktonic composition of POM influences its remineralization dynamics we developed a degradation experiment. First, we induced phytoplankton proliferations of different diatom contribution and then we followed the remineralization of the produced POM in the presence of mesopelagic prokaryotic communities.

To obtain POM of different composition, the surface water (<200 μm) was divided into ten 15-L plexiglass microcosms and incubated at 22°C with different inorganic nutrient enrichments and a 12:12 h light-dark cycle. Five microcosms were enriched with a nutrient solution to reach final concentrations of 23.1 μM of nitrate and 1.35 μM of phosphate; the NP incubation. The remaining five microcosms received the same nitrate and phosphate enrichment and an additional silicate solution (19.3 μM final concentration) to enhance diatom growth, the NPSi incubation (**Figure 1** – light incubations). Chlorophyll-a (Chl-a) concentration was measured daily to monitor the bloom development (**Supplementary Figure 1**) and inorganic nutrient concentrations were measured at the start and end of the incubations (**Supplementary Table 1**). The NPSi incubation was ended after 6 days, once Chl-a started decreasing. Due to the low Chl-a increase observed in the NP incubation (**Supplementary Figure 1**), and in order to achieve enough biomass for the degradation experiment, a second nitrate and phosphate solution was added to the NP incubation at day 6 and the collection of POM was postponed for 2 days. One day after the Chl-a maxima, all five microcosms of each light incubation were mixed and the particulate materials from NP and NPSi were collected by means of filtration (>0.6 μm, ipPORE 142 mm).

For the degradation experiment, all POM collected from each light incubation was resuspended into 60 L of 0.6 μm-filtered mesopelagic water: the resuspension of NP POM comprised the non-diatom dominated (non-DD) treatment, and the resuspension of NPSi POM was named the diatom dominated (DD) treatment (**Figure 1** – degradation experiment). Each treatment was distributed into three 20-L fluorinated carboys; one was used for the initial sampling and the other two served as experimental replicates during the 19 days of dark incubation at *in situ* mesopelagic temperature (14°C). Additionally, one carboy filled with mesopelagic water without any addition of particles was incubated as a control and sampled at the start and end of the experiment. A diagram of the experimental design can be found in **Figure 1**. All carboys used in the degradation experiment were filled with filtered mesopelagic water pooled from multiple containers at the start of the incubation and were gently stirred before every sampling to ensure homogeneous conditions.

Analytical Measurements

All labware used for sample manipulation, including sampling tubes and flasks, was acid-cleaned following the following rinsing sequence: Milli-Q water, 0.37% hydrochloric acid, 3× Milli-Q water, 3× water sample.

Chlorophyll-a concentration was determined using a Turner Designs fluorometer through the fluorometric method described by Yentsch and Menzel (1963). A volume of 100 ml sample was filtered through Whatman GF/F glass microfiber filter, the filter was kept in 90% acetone 24 h before the analysis. Identification and enumeration of phytoplankton was performed using the Utermöhl technique (Utermöhl, 1958). Briefly, samples were fixed with formalin-hexamine to a final concentration of 0.4% and stored at room temperature. Identification and enumeration were done on settled aliquots (10 ml) using an inverted microscope. Biomass calculations in terms of carbon used mean cell volumes per species obtained in previous studies (Arin et al., 2002a; Arin et al., 2002b; M. Delgado, personal communication) and the equations from Menden-Deuer and Lessard (2000) for vegetative cells, and from Kuwata et al. (1993) for *Chaetoceros* resting spores. Phytoplankton composition of the NP incubation was estimated using the mix of the five microcosms at the end of the incubation (1 day after the Chl-a maximum; **Supplementary Figure 1**). Due to the difficulty of identification and enumeration of phytoplankton in the mixed water from the NPSi incubation, we report the mean composition of the five microcosms 1 day before mixing (at the Chl-a maximum; **Supplementary Figure 1**).

Samples for inorganic nutrient analyses were collected unfiltered in duplicate polyethylene 12 ml tubes and stored at −20°C until analysis. Concentrations of phosphate (PO_4^{3-}), ammonium (NH_4^+), silicate (SiO_4^{2-}), nitrate (NO^{3-}), and nitrite (NO^{2-}) were determined using flow-through colorimetric methods in a Bran Luebbe AA3 AutoAnalyzer. Samples for POC, particulate organic nitrogen (PON) and particulate organic phosphorus (POP) were filtered onto pre-combusted (450°C for 4 h) Whatman GF/F filters and stored at −20°C until analysis. Carbon and nitrogen content was determined with a Perkin Elmer 2400 CNH analyzer. Filters for POC determination were decarbonated following the acid vapor method of Yamamuro and Kayanne (1995). Determination of POP was performed following the acid persulfate oxidation method described in Grasshoff et al. (1978). Dissolved organic carbon (DOC) samples were filtered through pre-rinsed 0.2 μm filters (Supor 200, Pall) and collected in duplicate into 30 ml polycarbonate flasks, positive pressure was applied during filtration with ultrapure N_2 gas and samples were stored at −20°C until analysis. DOC determination was carried out with a Shimadzu TOC VCSH instrument. Total

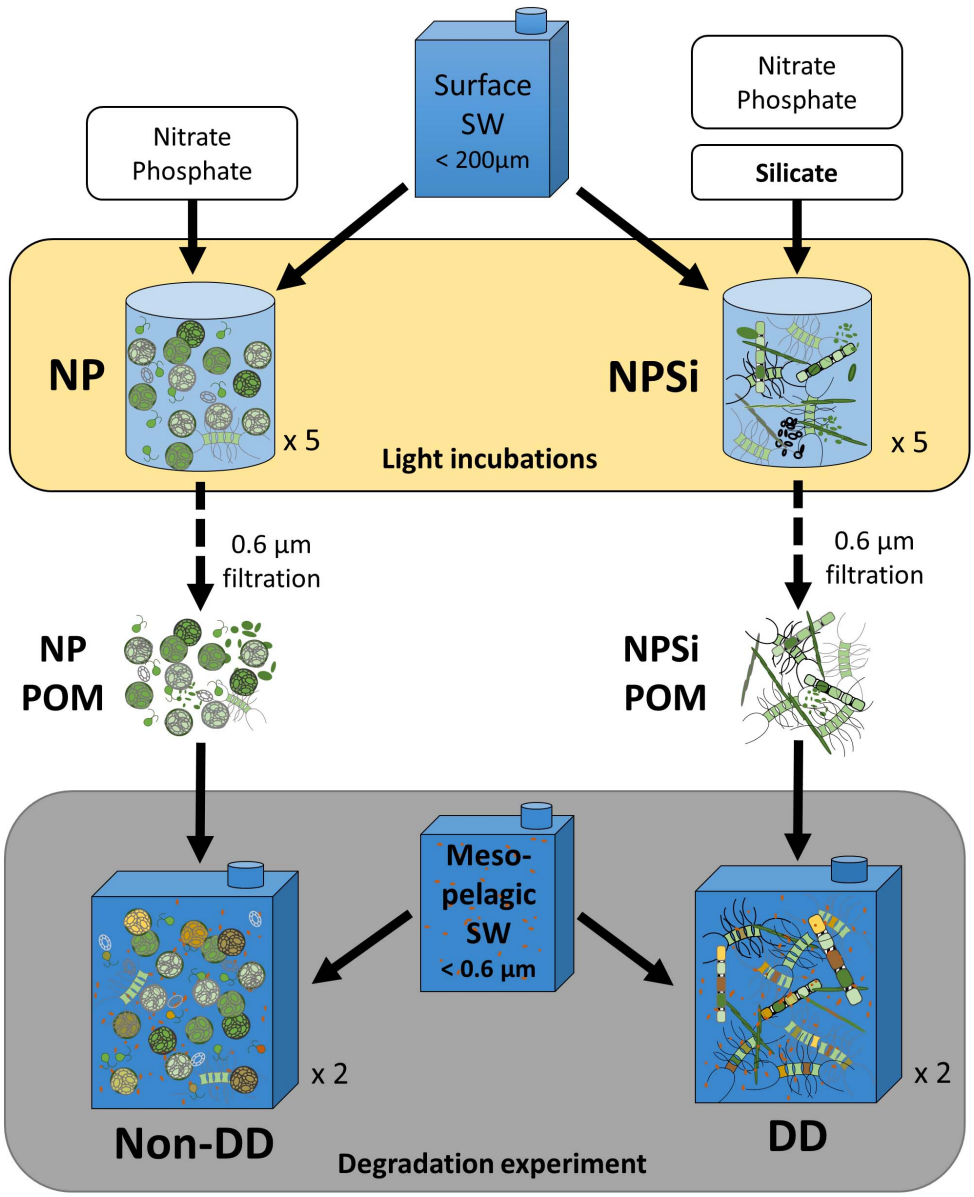

FIGURE 1 | Schematic representation of the experimental design. Light incubations (NP and NPSi) were used to induce phytoplankton proliferations of contrasting diatom dominance from a surface seawater sample enriched with different inorganic nutrient solutions. POM collected from the NP and NPSi incubations were each resuspended into mesopelagic seawater, comprising the two treatments of the degradation experiment: non-diatom dominated (non-DD) and diatom dominated (DD) treatments, respectively. The 19-day degradation experiment was performed in the dark at 14°C.

organic carbon (TOC) concentration was calculated as the sum of concentrations of POC and DOC.

Abundance of prokaryotes (hereinafter referred to as bacteria) was determined through flow cytometry (FC) using a BD FACSCalibur instrument. Samples were fixed with 1% paraformaldehyde plus 0.05% glutaraldehyde (final concentrations) and stored at −80°C until analysis. Samples were thawed and stained with SYBRgreen I at ∼ 20 µM final concentration at room temperature and in the dark for 10 min. Milli-Q was used as sheath fluid and the data acquisition was performed at a flow rate of approximately 18 µl min^{-1} for 2 min for each sample. Flow calibrations were performed before and after each batch of samples and the cell concentration was obtained by referring event counts to the daily mean flow. FC bacterial counts (**Supplementary Figure 4C**) were divided into two populations according to their nucleic acid content and size [as derived from red fluorescence and side-scatter (SSC), respectively]: high nucleic acid and low nucleic acid bacteria (**Supplementary Figures 4A,B**). We obtained population-specific cell volumes based on relative SSC signals (Calvo-Díaz and Morán, 2006), and conversions to bacterial biomass (BB) were performed using FC counts of each population and the

volume to biomass allometric model from Norland (1993): $C = 0.12\ V^{0.72}$, where C is cell biomass (pg C) and V is cell volume (μm^3). Bacterial production (BP) was determined following the ^{3}H-Leucine incorporation method (Kirchman, 2001).The C-specific BP was calculated by relating BP to BB.

Statistical Analysis

The degradation kinetics of phytoplankton-derived OC can be described with a first-order exponential decay model (Jewell and Mccarty, 1971):

$$OC_{(t)} = OC_{react}\ e^{-kt} + (1 - OC_{react})$$

where $OC_{(t)}$ is the fraction of initial OC remaining at time t, OC_{react} is the fraction of initial OC susceptible to degradation, the term (1 – OC_{react}) is the non-degradable fraction of initial OC and k is the rate of decomposition in d^{-1}. This first-order decay model has the advantage of k being insensitive to the initial OC concentration, which has been experimentally corroborated for phytoplanktonic degradation experiments with up to 30-fold differences in initial OC concentrations (Fujii et al., 2002).

We fitted this first-order decay model to the POC and TOC (DOC + POC) pools independently, using least square regressions of concentration vs time, to yield rate constants (k) and reactive fractions (OC_{react}) specific of each pool. Decay curve parameters were statistically compared between treatments and OC pools using extra sum-of-squares F test. We used this approach to test whether OC pools (TOC and POC) shared any decay parameters within each treatment (DD and non-DD) and to test whether the treatments shared any decay parameters of each OC pool.

RESULTS

Light Incubations: POM Production, Stoichiometry, and Phytoplankton Composition

The light incubations differed considerably in their POM production (**Table 1**); in terms of POC, the NPSi incubation was more than twice as productive as the NP incubation. POM stoichiometry, calculated as the molar ratio of the particulate constituents (POC, PON, and POP), was also substantially different between the two light incubations. POM from the incubation amended with silicate (NPSi) was richer in C and had a much lower C:Si ratio, calculated as the ratio between the final POC concentration and the apparent consumption (initial minus final concentrations) of dissolved silicate during the incubation.

The estimated phytoplankton community composition of the two light incubations is shown in **Figure 2**. The NPSi incubation produced a diatom-dominated community in which this group accounted for 98% of the biomass, including 47% in the form of *Chaetoceros* resting spores. The combined contribution of the other groups examined (i.e., coccolithophores, nanoflagellates, and dinoflagellates) made up the remaining 2% of the NPSi phytoplankton biomass. The phytoplankton community composition of the NP incubation was dominated by coccolithophores and nanoflagellates, accounting for 79 and 16% of the estimated phytoplankton biomass, respectively. The contribution of diatoms to NP phytoplankton biomass was estimated to be 6% and no diatom resting spores were detected. The total phytoplankton estimated biomass accounted for 97 ± 5% of the POC produced in the NPSi incubation and for 78 ± 3% in the case of the NP incubation.

TABLE 1 | Particulate organic carbon (POC) concentration (μM) and POM stoichiometry (mol:mol) at the end of the light incubations (NP and NPSi).

Incubation	POC	POM stoichiometry			
	(μM)	C:N	C:P	N:P	C:Si*
NP	79.6 ± 3.1	6.8 ± 0.3	83.8 ± 4.4	12.3 ± 0.7	142.2 ± 36.7
NPSi	171.6 ± 8.7	10.1 ± 0.5	175.4 ± 7.3	17.3 ± 0.4	9.8 ± 1.8

**Estimated ratio (see text). All variables are presented as mean ± standard deviation and were significantly different between incubations (at least $p < 0.05$, two-tailed t-tests, $n = 2$).*

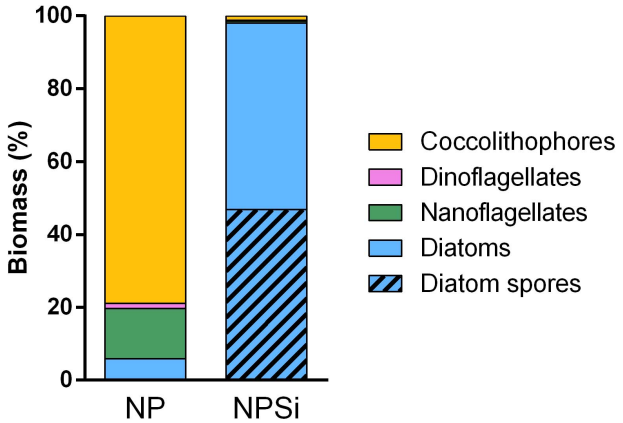

FIGURE 2 | Phytoplankton functional group composition (as percentage of estimated biomass) of NP and NPSi incubations.

Organic Carbon Dynamics

At the start of the experiment, immediately after the resuspension of POM from the light incubations into the mesopelagic water, DOC concentration of both treatments showed a sudden increase proportional to the added POC when compared to the mesopelagic water DOC (**Figure 3**). Then, DOC concentration of each treatment behaved differently; while DOC exhibited a consistent decrease in the non-DD treatment throughout the experiment, DOC concentration in the DD treatment experienced a pronounced initial drop and then it increased for the remaining of the experiment. Throughout the experiment, DOC concentration of both treatments remained above that of the mesopelagic water without the addition of particulate material, which showed no significant variation between the start and end of the experiment (t-test, $p = 0.33$).

Despite their different values at the beginning of the experiment, TOC concentrations followed remarkably similar

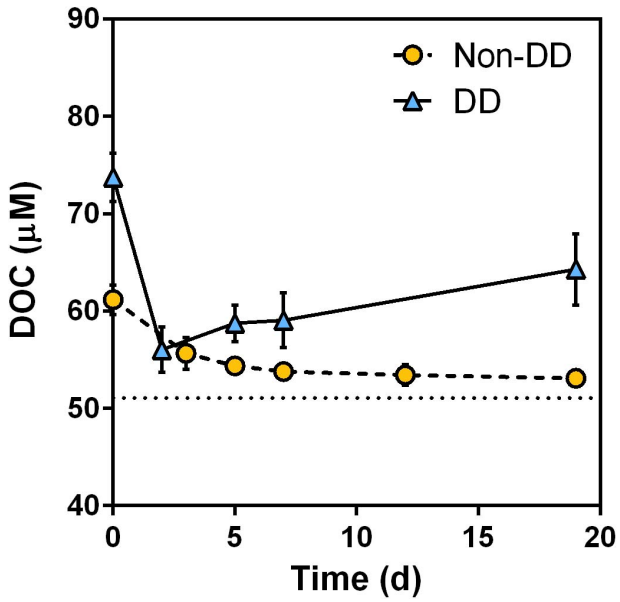

FIGURE 3 | Dissolved organic carbon (DOC) concentration during the experiment. Data are mean and standard deviation of two experimental replicates. Dotted line represents the concentration in the mesopelagic water prior to the POM additions.

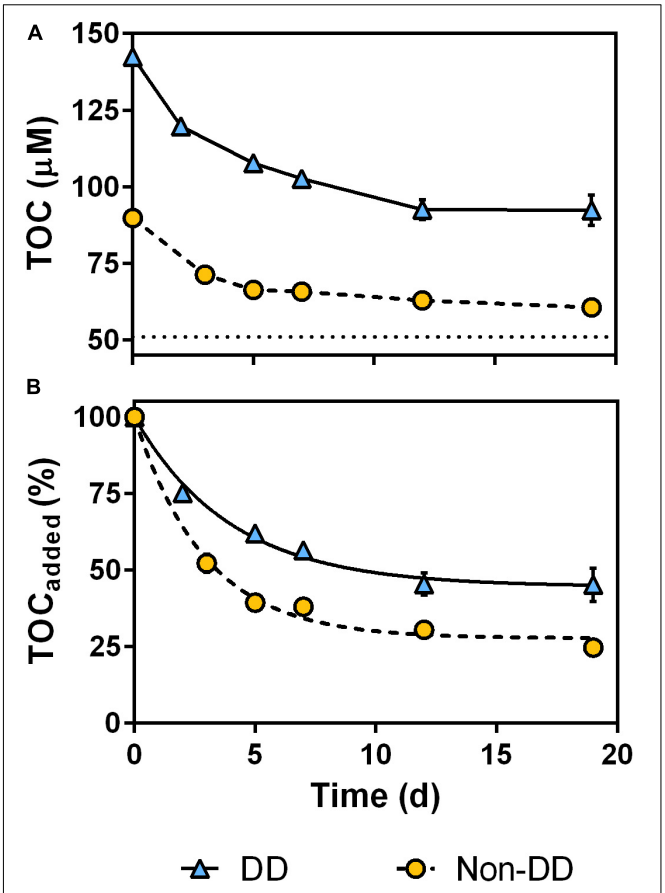

FIGURE 4 | Total organic carbon (TOC) decrease during the experiment, as absolute values **(A)** and as percentage of added TOC **(B)**. Data are mean and standard deviation of two experimental replicates; dotted line in **(A)** indicates DOC concentration of mesopelagic water prior to POM additions; solid and dashed lines in **(B)** are the best-fit decay curves for each treatment.

dynamics in both treatments (**Figure 4A**), decreasing rapidly during the first days and remaining more or less constant by the end of the experiment. When normalized to the added initial TOC (calculated as the difference between the initial TOC concentrations of the treatments and the mesopelagic water DOC), it becomes apparent that DD treatment TOC was remineralized at a slower rate and to a lesser extent than that of the non-DD treatment (**Figure 4B**), as denoted from the differences in the best-fit parameters of their decay curves (**Table 2**). TOC losses in each treatment showed statistically different degradation rates (k) and degradable fractions (OC_{react}).

Losses in POC concentration during the experiment (**Figure 5A**) behaved similarly to those observed for TOC (**Figure 4A**) in the non-DD treatment, with most of the degradation taking place within the first 5 days of the experiment. The DD treatment showed an overall slower decrease for POC than for TOC, with little decrease during the first 2 days of dark incubation and a similar loss during the first 7 days than during the remaining of the experiment (**Figure 5A**). Examining the POC losses relative to the respective initial concentrations of each treatment (**Figure 5B**) helps to appreciate how much faster POC was degraded in the non-DD treatment: the decay curve fitted for the non-DD treatment had a decay constant (k) that was three times higher than that of the DD treatment (**Table 2**). The fraction of degradable POC however, was similar between treatments. Model comparisons between the two OC pools in each treatment (**Table 2**) revealed that, in the non-DD treatment, TOC and POC kinetic parameters were not statistically different, whereas in the DD treatment each OC pool had different degradation rates (k) and degradable fractions (OC_{react}).

Stoichiometry of POM

Stoichiometry of POM, derived from concentrations of POC (**Figure 5A**), PON (**Figures 9A,B**), and POP (**Figures 9C,D**), showed important changes during the experiment in both treatments. The mean C:N ratio (**Figure 6A**) of the non-DD treatment remained stable with values in the range 7.75–7.84 for the first half of the experiment, increasing during the second half up to 9.42 at the end of the experiment. The mean C:N ratio of POM in the DD treatment showed a considerable drop at the beginning of the experiment and then it remained relatively stable with values in the range 6.93–7.89.

The mean C:P ratio (**Figure 6B**) of the non-DD treatment decreased during the first half of the experiment, increasing slightly during the second half. In the DD treatment, the ratio dropped at the beginning of the experiment from 180.0 ± 5.7 to 110.2 ± 0.2, it continued decreasing until the 7th day, and then raised until the end of the experiment.

The N:P ratio also exhibited variations (**Figure 6C**); the non-DD treatment experienced a decrease in its N:P ratio during the first half of the experiment from 11.7 ± 0.9 at the beginning to

TABLE 2 | First-order decay model best-fit parameters and significance of model comparisons for POC and TOC losses in the diatom dominated (DD) and non-diatom dominated (non-DD) treatments.

	Treatment	OC fraction	k (d^{-1})	OC_{react} (%)	Half-life (d)	S (%)
Best-fit	DD	TOC	0.25 ± 0.03	55.4 ± 1.9	2.78	3.01
		POC	0.10 ± 0.02	72.4 ± 8.1	6.93	4.69
	Non-DD	TOC	0.34 ± 0.03	72.3 ± 1.5	2.02	2.86
		POC	0.32 ± 0.03	70.2 ± 2.1	2.14	3.93
p-Values	DD vs non-DD	TOC	0.030	<0.001		
	DD vs non-DD	POC	<0.001	0.76		
	DD	TOC vs POC	<0.001	0.007		
	Non-DD	TOC vs POC	0.69	0.45		

Goodness of fit is given as standard error of regression (S).

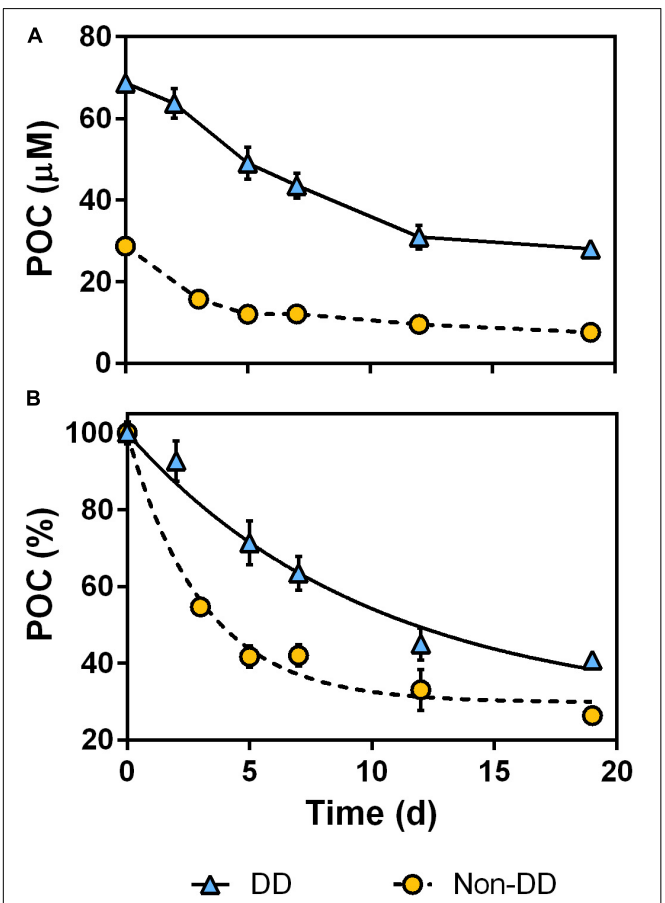

FIGURE 5 | Particulate organic carbon (POC) decrease during the experiment, as absolute values **(A)** and normalized to initial POC concentration of each treatment **(B)**. Data are mean and standard deviation of two experimental replicates, lines in **(B)** are first-order decay curves fitted for each treatment.

8.5 ± 0.3 on day 12. The mean N:P ratio of the DD treatment on the other hand decreased during the first 5 days of the experiment and then started to increase.

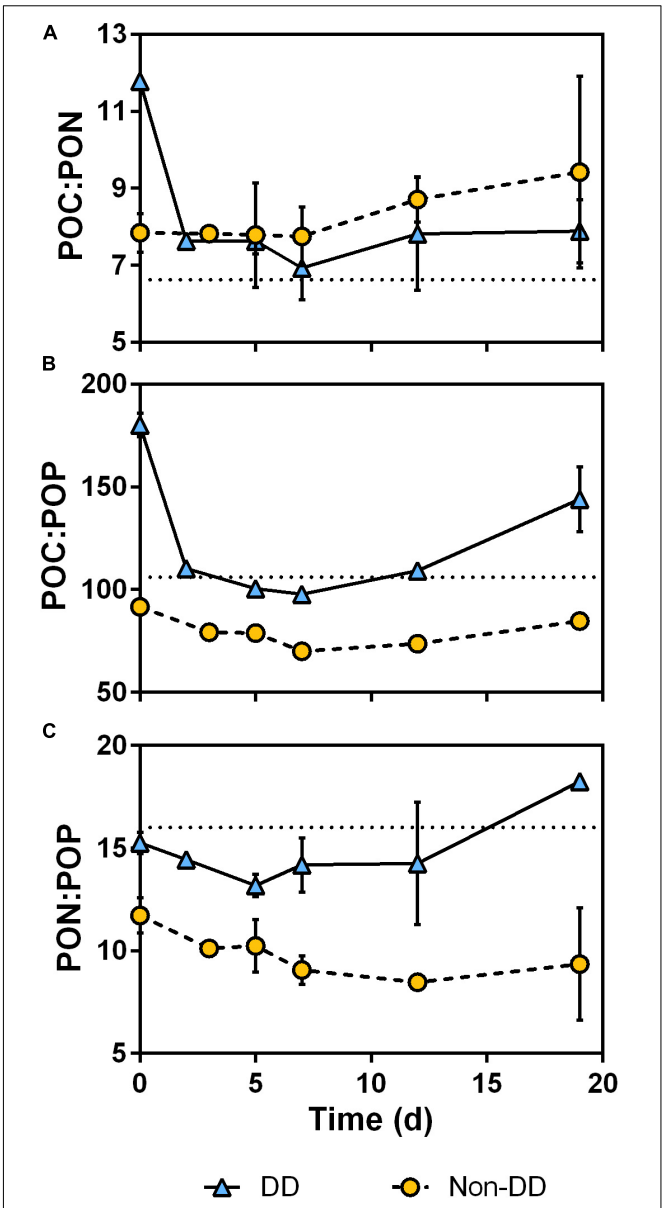

FIGURE 6 | Changes in POM mean C:N **(A)**, C:P **(B)**, and N:P **(C)** molar ratios during the experiment. Error bars are the standard deviation between two replicates. Dotted lines in each panel represent Redfield stoichiometric ratio (106C:16N:1P).

Nutrient Remineralization

The DD treatment exhibited a considerable drop in nitrate, phosphate, and silicate concentrations at the beginning of the experiment that was not detected in the non-DD treatment. Nitrate remained relatively stable for both treatments throughout the experiment, except for the aforementioned initial drop in the DD treatment (**Figure 7A**). Although a slight increase in nitrite concentrations was detected in both treatments (**Supplementary Figure 5**), their contribution to the nitrogen oxides pool was negligible (<3%). Both treatments started with a higher phosphate concentration than that of the

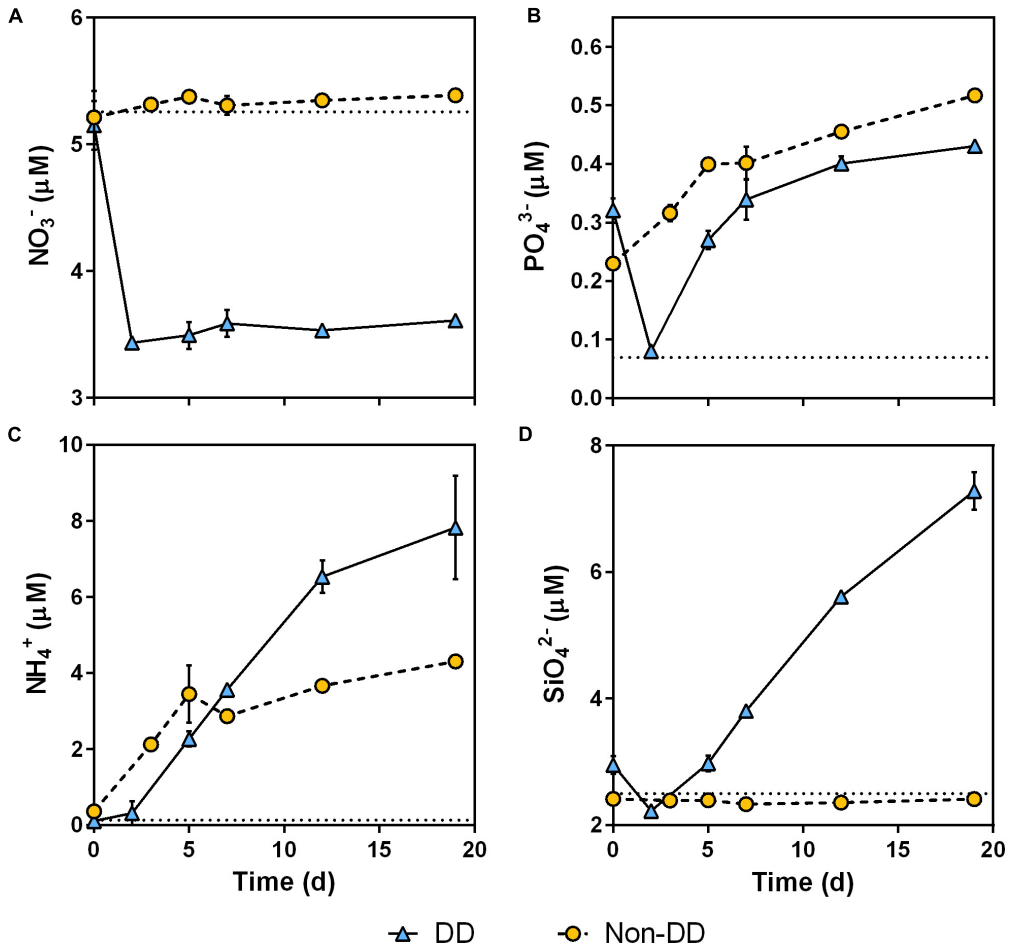

FIGURE 7 | Time-course of nitrate **(A)**, phosphate **(B)**, ammonia **(C)**, and silicate concentrations **(D)**. Data are mean and standard deviation of two replicates. Mean nutrient concentration of mesopelagic water prior to POM addition is shown in each panel as a dotted line.

mesopelagic water sample and then phosphate concentrations increased during the experiment in both treatments, with the DD treatment experiencing an initial drop in its phosphate concentration before increasing rapidly (**Figure 7B**). Ammonia concentrations increased consistently in both treatments (**Figure 7C**). Silicate concentration in the non-DD treatment remained unchanged throughout the experiment with respect to the silicate concentration of the sourced mesopelagic water sample (**Figure 7D**). In the DD treatment, the initial silicate concentration was slightly higher than that of the mesopelagic water sample prior to the addition of particulate material. This apparent excess of silicate was consumed at the beginning of dark incubation and then the silicate concentration increased at an apparent constant rate for the rest of the experiment (**Figure 7D**).

Bacterial Biomass and Production

Bacterial biomass (BB) behaved similarly in both treatments (**Figure 8A**), with one maximum at the beginning of the experiment, a substantial decrease at day 3 and then BB rose to a second maximum around the middle point of the experiment. The DD treatment exhibited higher BB values than the non-DD treatment throughout the experiment and, in both treatments, the BB started with values higher than those of the mesopelagic sample. The C-specific BP was higher in the non-DD treatment during the first half of the experiment, whereas the DD treatment exhibited higher values during the second half. Despite their different values, both treatments followed the same pattern in their C-specific BP: an initial increase from their initial values reaching the maximum after 3–5 days of incubation and then the C-specific BP dropped and remained low for the second half of the experiment (**Figure 8B**).

DISCUSSION

We have investigated the effects of phytoplankton community composition, specifically of diatom dominance, on the temporal dynamics of OM bacterial remineralization under controlled laboratory conditions. We have shown that phytoplankton community composition influenced the temporal dynamics of OM remineralization in several ways. First, POC derived from a

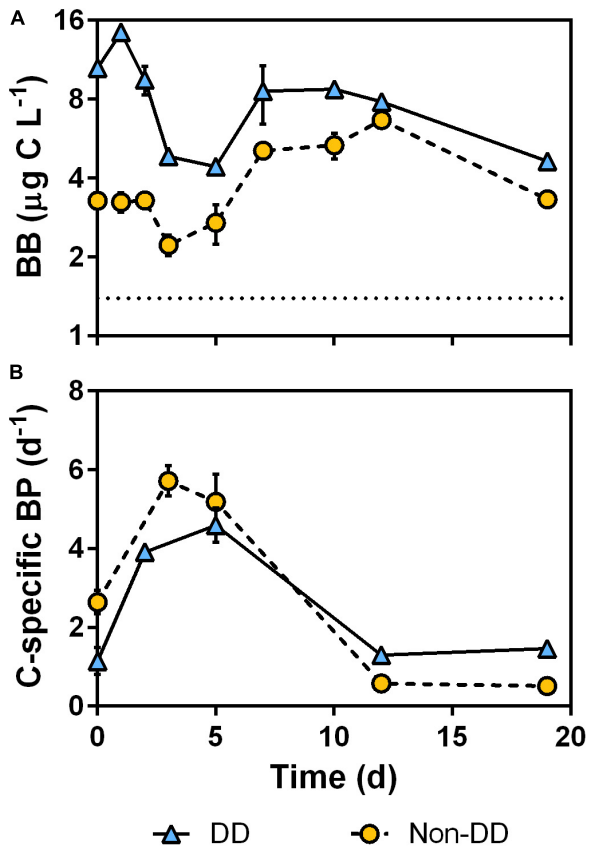

FIGURE 8 | Time-course of bacterial biomass **(A)** and C-specific bacterial production **(B)**. Data are mean and standard deviation of two experimental replicates. Mean bacterial biomass of mesopelagic water prior to POM addition is shown in **(A)** as a dotted line.

non-diatom-dominated community decayed much more rapidly (up to three times as fast) than that produced by one dominated by diatoms. Similarly, the TOC degradation rate was slower in the case of the diatom-dominated POM, possibly influenced by the accumulation of DOM of recalcitrant nature. Below we elaborate on possible explanations for these differences as well as on their significance in relation to the efficiency of the BCP, the biogeography of phytoplankton functional groups and the overall C-sequestration capacity of the ocean in the present and in future scenarios.

Light Incubations: POM Production, Stoichiometry, and Phytoplankton Composition

Diatom growth is favored when enough dissolved silica is available (Egge and Aksnes, 1992) and, as expected, this group predominated in the containers amended with silicate (NPSi). In addition, the higher growth rates attributed to diatoms (Marañón et al., 2013) probably contributed to the higher POM production observed in the NPSi incubation. The higher POM C:N and C:P ratios in the NPSi incubation could be due to increased production and accumulation of carbon-rich lipids (Breuer et al., 2012; Yang et al., 2013) and/or carbohydrates (Guerrini et al., 2000; Chauton et al., 2013) under the N-limiting conditions experienced at the end of the NPSi incubation (**Supplementary Table 1**). This nutritional deficiency appears to have induced the production of diatom resting spores (Oku and Kamatani, 1997), which accounted for a substantial fraction (47%) of the phytoplankton biomass in the NPSi incubation. Although the usage of the volume-to-C factor from Kuwata et al. (1993) for *Chaetoceros* spores can lead to overestimations of the contribution of resting spores to total phytoplankton biomass (Rynearson et al., 2013), the good agreement between NPSi estimated phytoplankton biomass (167 µmol C L^{-1}) and measured POC (172 ± 9 µmol C L^{-1}) gives us confidence in the appropriateness of its use in our case. The abundance of C-dense resting spores helps explain the high C:N and C:P ratios of the POM produced in the NPSi incubation (**Table 1**).

In the NP incubation, coccolithophores had a substantial contribution although they were not as dominant as diatoms were in the NPSi incubation (**Figure 2**). The low contribution of diatoms to the estimated NP biomass (6%) is probably a lower limit estimate, as the state of diatoms at the end of the NP incubation made their identification and enumeration challenging. This probably contributed to the mismatch between estimated phytoplankton biomass (62 µmol C L^{-1}) and measured POC concentration (80 ± 3 µmol C L^{-1}). The "aged" appearance of diatoms in the NP incubation indicates that the succession of phytoplankton functional groups played an important role in the bloom dynamics of this incubation. In fact, earlier samples of NP incubation had a much higher diatom contribution (**Supplementary Figure 2**). Diatoms, which outcompete coccolithophores under pulsing nutrient supply dynamics (Cermeño et al., 2011), would have better exploited the initial nutrient addition and dominated the production in the NP incubation production until silicate was exhausted, when coccolithophores would have been able to increase their dominance.

Nutrient Remineralization

At the start of the experiment, the apparent consumption of nitrate (**Figure 7A**) and phosphate (**Figure 7B**) in the DD treatment could be attributed to prokaryotic uptake. When limited by organic nutrients, bacteria have been reported to compensate this deficiency by incorporating inorganic forms of N and P, which allows them to further utilize nutrient poor OM (Kragh et al., 2008), such as that produced on the NPSi incubation (**Table 1**). The synchronous consumption of silicate (**Figure 7D**) in this treatment, however, points to diatoms still being actively taking up nutrients at the very beginning of the degradation experiment. The ability of diatoms to incorporate inorganic nutrients into particulate material upon the first 24–48 h of darkening has been reported previously in similar degradation experiments (Blank and Sullivan, 1979; Passow et al., 2011). The nutrient stress experienced by the phytoplankton community at the end of the NPSi light incubation (**Supplementary Table 1**) probably caused an enhanced uptake of N, P, and Si by diatoms when transferred to the relatively nutrient-rich mesopelagic water. Although some prokaryotic uptake cannot be completely

ruled-out, the nutrient-stressed diatoms, which outweighed bacteria 80 to 1 in terms of biomass, are probably responsible for the bulk of the nutrient consumption observed at the start of the experiment. The initial uptake of nutrients by diatoms affected POM composition severely in the DD treatment, with losses of dissolved inorganic N and P being balanced by concomitant increases in PON and POP (**Figures 9B,D**, respectively). This reduced the initial C:N and C:P ratios to values more similar to those of Redfield by the second day of the experiment (**Figures 6A,B**, respectively).

The absence of a similar nutrient consumption in the non-DD treatment could be either due to phytoplankton being too damaged to still be active or to having its inorganic nutrient requirements already satisfied. The low C:N and C:P ratios of the POM from the NP incubation (**Table 1**) and the relatively high inorganic nutrient concentration at the end of this light incubation (**Supplementary Table 1**) supports the second explanation. After the second day of the experiment, the silicate concentration in the DD treatment increased at a fairly constant rate throughout the rest of the experiment, evidencing diatom frustule dissolution in agreement with previous degradation experiments (Passow et al., 2011) in which silica dissolution behaved linearly with time.

Total Organic Carbon Dynamics

Decay of phytoplankton-derived OM is sometimes modeled to follow multiple first order kinetics in which various OM fractions with different reactivities are considered (Multi-G model, e.g., Sempéré et al., 2000), which agrees with the conceptual model of OM size-reactivity continuum (Benner and Amon, 2015). Modeling studies can use an infinite number of OM pools characterized by a continuous distribution of reactivities to best describe the complex nature of OM (Aumont et al., 2017). In experimental approaches, however, a single decay rate is usually computed for the sake of simplicity (Goutx et al., 2007; Engel et al., 2009), as the differentiation of even a few discrete OM pools with different reactivity requires a high frequency sampling strategy that is usually difficult to achieve due to sample volume constrains. Thus, we used a single first-order decay model for each treatment that yielded an overall good fit to our data and low standard errors of the model parameters (**Table 2**). Although the remineralization rates presented here are influenced by our experimental design and choice of model, and should not be extrapolated directly to field data, we deem this approach appropriate for comparative purposes between treatments.

The rapid decrease of DOC in the DD treatment within the first 2 days of the experiment (**Figure 3**) was partially compensated by the reduced apparent consumption of POC over the same period (**Figure 5**). This could be the result of re-aggregation processes, through which part of the DOC adheres to particles big enough to be retained during the filtration of POC, and/or of preferential degradation of fresh DOM over POM by the prokaryotic community. Similarly, the loss of POC concentration overtime in the DD treatment was partially counteracted after the second day of the experiment by the accumulation of DOC. This increase could be attributed to the release of recalcitrant DOM as a by-product of POM degradation, which would be in agreement with previously reported increases of low molecular weight DOM during degradation of diatom particles (Hama et al., 2004). The evolution of some DOM optical indices measured during our experiment, such as the absorption ratio a300:a400 and DOC-normalized humic fluorescence (**Supplementary Figure 3**), support this explanation. The absence of a similar DOC accumulation in the non-DD treatment could be a consequence of the higher POM lability observed in this treatment. In this scenario, the microbial community would have been able to degrade non-DD POM further, respiring most of its C and releasing only a minor fraction as recalcitrant DOM. This OM dynamics would be represented by the slight difference in the final DOC concentration between the non-DD treatment and that of the mesopelagic water prior to the addition of particles (**Figure 3**).

Transfer of OC between the particulate and dissolved fractions appears to have compensated the slight discrepancies in the expected POC dynamics of the DD treatment, yielding a decay pattern of the combined TOC pool that fits the expected first order kinetics better than the particulate fraction alone (**Table 2**). Overall, the non-DD treatment OM decayed faster than that of DD, as denoted by the higher TOC remineralization rate of the non-DD treatment. Moreover, the extent of the degradation process was also higher for the non-DD treatment, with $75 \pm 2\%$ of the added TOC being degraded over the 19 days of dark incubation. The lower relative loss of TOC in the DD treatment throughout the experiment was probably due to the accumulation of recalcitrant DOC, which limited OM remineralization in this treatment to $55 \pm 5\%$ of the TOC added to the mesopelagic water.

Particulate Organic Carbon Dynamics

The different rates of POC remineralization exhibited by each treatment during the experiment point to DD treatment POM being less labile than that of the non-DD treatment. Two main, non-mutually exclusive factors could be playing a role in this result: (i) differences in POM chemistry between treatments and/or (ii) the protective effect of diatom frustules against bacterial decomposition in the DD treatment.

POM Chemical Composition

Mediterranean microbial communities have been consistently reported to be P-limited, both at surface (Thingstad et al., 1998; Pinhassi et al., 2006) and at depth (Sala et al., 2002; Van Wambeke et al., 2002). Due to the relatively low phosphate concentration (0.070 ± 0.005 μM PO_4^{3-}) and high inorganic nutrient N:P ($\sim$ 83:1) of the mesopelagic water sample used in the experiment, we expected the bacterial community to be P-limited. Bacterial metabolism depends on substrate stoichiometry, with lower C:N and C:P of organic substrates leading to higher BP and growth efficiency (Kroer, 1993; Lennon and Pfaff, 2005). Thus, POM phosphorus content was expected to have a considerable impact on bacterial activity and their growth capabilities in our experiment.

The coccolithophore-dominated NP incubation was comparatively less efficient in carbon production, which resulted in POM relatively rich in nitrogen and, especially, in phosphorus as denoted from POM stoichiometry. Meanwhile,

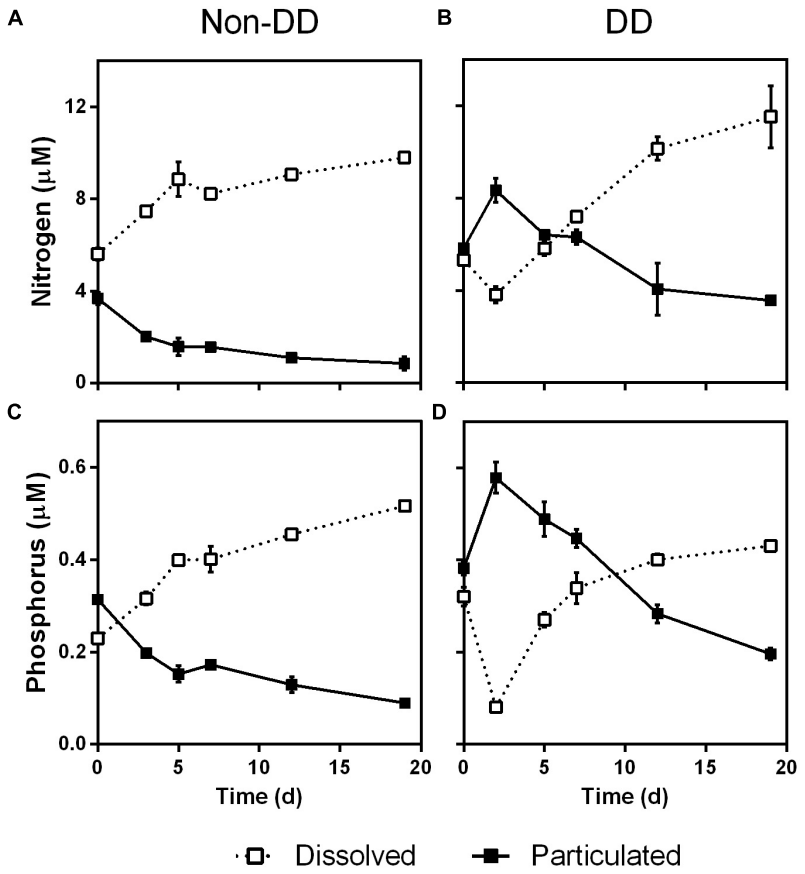

FIGURE 9 | Time course of nitrogen **(A,B)** and phosphorus fractions **(C,D)** for the non-DD **(A,C)** and DD **(B,D)** treatments. Dissolved fractions are inorganic forms of N (ammonia, nitrate, and nitrite) and P (phosphate); particulated fractions are PON and POP. Data are mean and standard deviation of two experimental replicates.

the NPSi incubation produced relatively C-rich POM, with higher C:N and C:P ratios (**Table 1**). Even after the considerable initial drop in the DD treatment POM C:N and C:P ratios, which has been discussed previously, non-DD POM remained P-rich in comparison, with lower C:P and N:P ratios for the rest of the experiment (**Figures 6B,C**, respectively). This high phosphorus POM content might have alleviated bacterial P limitation and stimulated its growth in the non-DD treatment, accelerating the POC consumption in this treatment relative to that of the DD treatment.

Particulate organic matter stoichiometry varied throughout the experiment hinting toward expected prokaryotic nutritional requirements: During the first 5–7 days both treatments experienced a decline in C:P and N:P ratios of POM (**Figures 6B,C**, respectively), indicating preferential remineralization/dissolution of C and N over P. This would be in agreement with the expected requirements of a prokaryotic community in lag-phase, building up enzymatic machinery while adapting to the high resource environmental conditions (Madigan et al., 1997). This "adaptation" period would have been accompanied by the loss of the bacterial community transferred from the light incubations, as denoted by the drop in BB observed in both treatments, DD and non-DD, after the second day of the experiment (**Figure 8A**). After day 7, increasing POM C:P ratios indicate an enhanced P remineralization relative to that of C (**Figure 6B**). The increase in BB after the initial drop is consistent with the expected growth of the original mesopelagic bacterial community in response to the decay of bacteria from the light incubations (**Figure 8A**).

Additionally, chemical characteristics of POM other than stoichiometric differences could have influenced POM degradation kinetics in our experiment. In a revision of phytoplankton macromolecular composition, Finkel et al. (2016) identified significant differences between phyla of microalgae in their proportions of proteins, carbohydrates and lipids. To date, a universal ranking of these compounds labilities remains elusive for marine POM (Benner and Amon, 2015), with different studies reporting variable labilities depending on their POM source and degradation conditions (Harvey et al., 1995; Harvey and Macko, 1997; Panagiotopoulos et al., 2002; Goutx et al., 2007). However, we cannot dismiss the possibility that the compositional differences of phytoplanktonic POM have influenced the degradation dynamics observed in this experiment. Further research is required to determine the link between POM chemical composition and its remineralization kinetics.

Mineral Cover Protective Effects

Diatom silica frustules have been reported to provide protection against diverse threats to cell integrity, such as UV radiation (Ellegaard et al., 2016) grazing (Hamm et al., 2003; Assmy et al., 2013) or viral infection (Kranzler et al., 2019). Protection of diatom POM from bacterial degradation by silica frustules has been also reported by Moriceau et al. (2009), who observed an enhanced degradation rate constant of POC once enough biogenic silica had been dissolved. During degradation, heterotrophic prokaryotes have to first attack the organic matrix of the frustules via the secretion of extracellular hydrolases, exposing the underlying silica to dissolution into the undersaturated surrounding water. The bacterial-mediated dissolution of silica frustules (Bidle and Azam, 1999) represents an extra step, which makes diatom POM harder to degrade relative to that of non-silicifying phytoplanktonic groups. This protective effect can be specially relevant for the preservation of resting spores, whose heavily silicified frustules allow them to persist degradation and dominate deep POC fluxes in some cases (Rembauville et al., 2016). Assuming that the increase of silicate concentration in the DD treatment accounts for all biogenic silica dissolution, and using the C:Si ratio calculated for NPSi POM, we expect the dissolution of silica in the DD treatment to have exposed 42 $\pm$ 7 μM of POC throughout the experiment. This estimation matches well with the amount of POC remineralized in the DD treatment during the experiment (40.7 $\pm$ 0.7 μM), which could be a strong indication that this mechanism has limited to some extent the POM degradation of this treatment.

Whereas diatom POC can remain within senescent and intact dead cells, coccolithophore cell POC and coccolith PIC separate readily after cell death (De La Rocha and Passow, 2007). This is further supported by multiple experimental observations of net detachment of coccoliths at low growth rates and especially at stationary phase (Balch et al., 1993; Fritz and Balch, 1996; Fritz, 1999). Thus, it is reasonable to assume that coccoliths may have not provided as much protection to coccolithophores against bacterial activity in the non-DD treatment as opal frustules did to diatoms in the DD treatment.

The Role of Diatoms and Coccolithophores in the Global C Cycle

Diatoms and coccolithophores are two of the most prominent players in carbon export, collectively responsible for approximately 50% of POC export (Jin et al., 2006) as mineral-ballasted, bloom-forming phytoplankton functional groups. However, the chemical nature of their mineralized cell walls can modulate the net effect of their blooms on atmospheric CO_2 drawdown. Coccolithophore calcification has an opposite effect to their photosynthetic C fixation by reducing the alkalinity of surface waters and thus decreasing the ocean storage capacity for CO_2 (Rost and Riebesell, 2004). Consequently, coccolithophore blooms have a reduced carbon sequestration potential when compared to non-calcifying phytoplankton proliferations (Boyd and Trull, 2007). Ultimately, the C-sequestration of a given system depends on the BCP efficiency, described by two metrics: particle export efficiency (PE_{eff}), defined as the proportion of NPP that is exported from the sunlit layer of the ocean; and transfer efficiency (T_{eff}), the fraction of organic export that reaches the deep ocean (Henson et al., 2012).

Contrasting export- and transfer-efficiency patterns have been observed consistently in regions dominated by either coccolithophores or diatoms (Francois et al., 2002; Lam and Bishop, 2007; Henson et al., 2012). Coccolithophore-dominated regions exhibit low PE_{eff} but little loss of exported material with depth (i.e., high T_{eff}), whereas regions dominated by diatoms show relatively high PE_{eff} but intense attenuation of POC flux thereafter (low T_{eff}). In our experiment, we observed contrasting temporal dynamics in POC concentrations (**Figure 5A**) and C-specific BP between treatments (**Figure 8B**) that agree with the patterns in remineralization length scale described above. During the first 5 days of the experiment, the coccolithophore-dominated non-DD treatment experienced a higher relative POC loss (60%) than the diatom-dominated DD treatment (30%) and supported higher C-specific BP. After the fifth day, however, we found the opposite pattern, with the non-DD treatment losing a further 15% of its initial POC and supporting less C-specific BP than the DD treatment, which lost an additional 30% of its initial POC in the same period. Other things being equal (i.e., sinking rates), these spatio-temporal patterns imply that a greater fraction of remineralization occurs in deeper waters for diatom-dominated assemblages, increasing their C sequestration potential (Kwon et al., 2009).

The overall slower degradation rates of diatom-derived material found in our experiment is consistent with field observations of phytoplankton taxonomic composition and degradation markers of deep ocean samples. Agusti et al. (2015) found that diatoms dominate phytoplanktonic assemblages found in the deep ocean (2000–4000 m) at tropical and subtropical latitudes, and that their dominance increased at depth with respect to the overlying surface communities. Ingalls et al. (2006), who compared the degradation state of 1000 m sediment trap materials in the Southern Ocean based on amino acid and pigment compositions, found the highest degree of degradation at sites with high coccolithophore contribution, whereas diatom-dominated stations showed little signs of bacterial degradation. Furthermore, the sedimentary record shows a widespread dominance of diatom remains, especially resting diatom spores, in marine sediments underneath some of the most productive coastal upwelling systems of the world (Abrantes et al., 2016). These observations suggest that diatoms are better equipped than other phytoplanktonic groups to endure the transit through the mesopelagic ocean and withstand microbial degradation.

Much uncertainty remains on how different environmental factors and biotic interactions control present and future phytoplankton biogeography patterns (Cermeño et al., 2008; Boyd et al., 2010). However, some studies point to a diminishment of diatom contribution due to global change: In coastal regions influenced by large river discharge, various anthropogenic impacts are disturbing nutrient stoichiometry inputs toward lower relative concentrations of silicate (Turner et al., 2003; Garnier et al., 2010), forcing phytoplankton assemblages toward lower diatom contribution and concurrent lower C-export (Turner et al., 1998). In

open ocean environments, some observations hint toward an expanded geographical distribution of coccolithophores in regions historically dominated by diatoms, as temperature and ocean stratification increases due to climate change (Merico et al., 2003; Cubillos et al., 2007; Cermeño et al., 2008). Based on the differences discussed in the previous paragraphs and the overall higher lability of coccolithophore POM found in our experiment, the projected shifts from diatom- to coccolithophore-dominated communities may hinder the oceans atmospheric CO_2 drawdown through a reduced efficiency of the BCP.

Experimental Approach Limitations

Although it is not feasible to reproduce all conditions experienced by phytoplankton aggregates during their journey through the water column, degradation experiments can provide useful information on the different processes at play in the degradation of POM. Here, we examined the effect of POM photosynthetic origin on its degradation dynamics in terms of carbon removal rates and changes in stoichiometry. To focus on this effect, we excluded other sources of variability that otherwise could have influenced the degradation process as described in M&M. Still, we identified some patterns that may have been caused by the unavoidable artifacts of the experimental design and will be discussed here.

At the beginning of the experiment, the discrepancies in DOC and phosphate concentrations between the mesopelagic water and the initial samples of each treatment (**Figures 3**, **7B**, respectively) could be linked to the mechanical resuspension of the particulate material, which may have caused cell lysis and released intracellular contents to the mesopelagic water. The absence of a similar increase in nitrogen is probably due to differences in P and N cell allocation, with N mostly contained in macromolecules that require specific enzymes to be hydrolyzed, while a large fraction of P can be found in storage structures that require little biological activity to be released (Liefer et al., 2019). These findings are in agreement with those from Burkhardt et al. (2014), who described P abiotic solubilization but virtually no N release within minutes of resuspension of phytoplanktonic POM. We also found discrepancies between the initial BB of each treatment, and that of the mesopelagic sample (**Figure 8A**). This apparent excess in BB indicates that the collection of particulate material from the light incubations on the filters also retained a substantial fraction of the bacterial community associated with the phytoplankton blooms. The drop observed in BB of both treatments after the second day of the experiment is probably due to the death of part of the bacterial community transferred from the light incubations. These patterns were found in both the non-DD and DD treatments, and the discrepancies in concentrations of different components were proportional to the added particulate material of each treatment, making the degradation process comparable between treatments even though extrapolation of results from this experiment should be taken with caution. The main goal of the experiment, however, was not to obtain specific rates of remineralization but to characterize the effect of phytoplankton community composition and physiological state on the OM bacterial degradation process.

We consider that the filtration of mesopelagic water prior to the start of the experiment may have excluded part of the particle-attached mesopelagic prokaryotes, however, we believe that the need to exclude any uncharacterized particles and bacterial grazers, which might otherwise have influenced the results, justified this action. We also evaluated the possibility of microbial oxygen limitation impacting our results using raw conservative calculations of oxygen consumption during OM respiration (**Supplementary Methods**). We estimated that, throughout the experiment, the dissolved oxygen concentrations decreased from 255 to 198 $\pm$ 6 and 222 $\pm$ 1 μM in the DD and non-DD treatments, respectively. These oxygen consumptions translate into minimal decreases of microbial respiration (2.9 $\pm$ 0.4 and 1.6 $\pm$ 0.0% in the DD and non-DD treatments, respectively). In addition, the containers were ventilated in every sampling, since this aeration was not included in our calculations, we can conclude that oxygen limitation was minimal.

In our experimental setup, we purposely excluded large (>200 μm) zooplanktonic grazers at the beginning of the POM production incubations to allow for relatively fresh phytoplanktonic POM to be collected for the degradation experiment. Although simplistic, this would be representative of high-export conditions of decoupled productivity and grazing. In cases where primary producers escape zooplankton grazing and rapidly sink out of the euphotic zone such as rapidly growing blooms (Cadée, 1985; Dünweber et al., 2010; Martin et al., 2011) and fast export pulses due to subduction events (Omand et al., 2015; Thomsen et al., 2017), the patterns found in this study should apply.

Future Research Challenges

Obtaining a better understanding of the linkage between plankton ecophysiology, export production and POC attenuation with depth is crucial to inform models and improve our ability to predict the roles of the BCP and the MCP in future ocean scenarios. In this study, we have identified some knowledge gaps that might help guide future studies that aim to quantify and model POM degradation rates.

The release of DOM during bacterial degradation of POM may represent an important fraction of POC losses and it should be taken into account to avoid overestimations of POC respiration. Accumulation of RDOM during bacterial degradation of phytoplanktonic POM has only been described, to the best of our knowledge, in experiments involving diatom materials (Lara and Thomas, 1995; Hama et al., 2004). Similarly, we found that DOM release and accumulation was much more prominent during the degradation of diatom-derived POM. Low-labile DOM can serve as a very effective C storage pool (Jiao et al., 2010) and more studies are required to elucidate how phytoplankton community composition influences the production of RDOM.

The formation of resting spores allows diatoms to persist unfavorable conditions procuring them with a standing stock of semi-dormant cells that can react relatively rapidly when conditions improve. As a side-effect, their C-rich nature and highly silicified frustules make this resting cell forms optimal vectors for C-export, dominating deep POC fluxes in some cases.

Unfortunately, the lack of specific volume-to-C estimates for many species makes obtaining accurate quantification of their importance in terms of C challenging (Rynearson et al., 2013). Our ability to understand the impact of resting spores on the efficiency of the BCP would benefit from detailed studies of spore physiology and biochemical composition.

The striking differences in POM remineralization rates found in our experiment are probably the result of additive and/or synergistic effects of POM stoichiometry, mineral cover protection and phytoplanktonic origin. Future studies evaluating the individual and combined effects of each of these factors on the dynamics of bacterial decomposition of phytoplanktonic materials will allow us to improve predictive models of the oceanic C-cycle. Likewise, quantifying the contribution of zooplankton and prokaryotes to POM remineralization as a function of the phytoplankton community composition should be a priority, as it will help us elucidate the extent of the impact that the differences in resistance to bacterial degradation described in this study have on the efficiency of the BCP.

CONCLUSION

We have shown that the dynamics of POM bacterial remineralization is strongly dependent on its phytoplanktonic origin. When compared to non-diatom phytoplankton proliferations, diatom POM was degraded to a lower extent and at a much slower rate over the 19-day degradation experiment. In addition, bacterial processing of diatom POM resulted in the release and accumulation of DOM of tentative recalcitrant nature. Overall, these results suggest that projected declines in diatom dominance due to global change might lead to a greater lability of export production and reduced efficiencies of the BCP and the MCP.

DATA AVAILABILITY STATEMENT

The raw data supporting the conclusions of this article will be made available by the authors, without undue reservation.

AUTHOR CONTRIBUTIONS

MC-B, PC, and CM: experimental design and interpretation and discussion. MC-B, LA, MS, and CM: source water sampling. MC-B, LA, and MS: sample analysis. MC-B: manuscript writing. All authors: experiment execution, and revision, correction, and approval of final manuscript.

FUNDING

This research was funded by projects SUAVE (CTM2014-54926-R), ANIMA (CTM2015-65720-R), and BIOGAPS (CTM2016-81008-R) and the institutional support of the "Severo Ochoa Centre of Excellence" accreditation (CEX2019-000928-S) from the Spanish government. MC-B was supported by a FPU pre-doctoral contract (FPU16/01925) from the Spanish government. We acknowledge support for the publication fee by the CSIC Open Access Publication Support Initiative through its Unit of Information Resources for Research (URICI).

ACKNOWLEDGMENTS

The authors would like to thank the captain, crew, and technicians of the R/V García del Cid and the colleagues who participated in the AMICS expedition and helped with the experiment execution (Idaira Santos, Yaiza Castillo, Carolina Antequera, Francesc Peters, and Lluïsa Cros). Inorganic nutrient analyses were performed by M. I. Abad in coordination with E. Berdalet (Head of the Service) at the "Nutrient Analysis Service" of the ICM-CSIC. The authors also thank Marta Estrada and Josep M. Gasol for their valuable comments and insights during the interpretation and writing of this study.

SUPPLEMENTARY MATERIAL

The Supplementary Material for this article can be found online at: https://www.frontiersin.org/articles/10.3389/fmars.2021.683354/full#supplementary-material

REFERENCES

Abrantes, F., Cermeño, P., Lopes, C., Romero, O., Matos, L., Van Iperen, J., et al. (2016). Diatoms Si uptake capacity drives carbon export in coastal upwelling systems. *Biogeosciences* 13, 4099–4109. doi: 10.5194/bg-13-4099-2016

Agusti, S., González-Gordillo, J. I., Vaqué, D., Estrada, M., Cerezo, M. I., Salazar, G., et al. (2015). Ubiquitous healthy diatoms in the deep sea confirm deep carbon injection by the biological pump. *Nat. Commun.* 6:7608. doi: 10.1038/ncomms8608

Anderson, T. R., and Tang, K. W. (2010). Carbon cycling and POC turnover in the mesopelagic zone of the ocean: insights from a simple model. *Deep. Res. Part II Top. Stud. Oceanogr.* 57, 1581–1592. doi: 10.1016/j.dsr2.2010.02.024

Arin, L., Marrasé, C., Maar, M., Peters, F., Sala, M., and Alcaraz, M. (2002a). Combined effects of nutrients and small-scale turbulence in a microcosm experiment. I. Dynamics and size distribution of osmotrophic plankton. *Aquat. Microb. Ecol.* 29, 51–61. doi: 10.3354/ame029051

Arin, L., Morán, X. A. G., and Estrada, M. (2002b). Phytoplankton size distribution and growth rates in the Alboran Sea (SW Mediterranean): short term variability related to mesoscale hydrodynamics. *J. Plankton Res.* 24, 1019–1033. doi: 10.1093/plankt/24.10.1019

Aristegui, J., Duarte, C. M., Agustí, S., Doval, M., álvarez-Salgado, X. A., and Hansell, D. A. (2002). Dissolved organic carbon support of respiration in the dark ocean. *Science* 298, 1967–1967. doi: 10.1126/science.1076746

Assmy, P., Smetacek, V., Montresor, M., Klaas, C., Henjes, J., Strass, V. H., et al. (2013). Thick-shelled, grazer-protected diatoms decouple ocean carbon and silicon cycles in the iron-limited Antarctic Circumpolar Current. *Proc. Natl. Acad. Sci. U.S.A.* 110, 20633–20638. doi: 10.1073/pnas.1309345110

Aumont, O., Van Hulten, M., Roy-Barman, M., Dutay, J. C., Éthé, C., and Gehlen, M. (2017). Variable reactivity of particulate organic matter in a global ocean biogeochemical model. *Biogeosciences* 14, 2321–2341. doi: 10.5194/bg-14-2321-2017

Bach, L. T., Boxhammer, T., Larsen, A., Hildebrandt, N., Schulz, K. G., and Riebesell, U. (2016). Influence of plankton community structure on the sinking velocity of marine aggregates. *Glob. Biogeochem. Cycles* 30, 1145–1165. doi: 10.1002/2016GB005372

Bach, L. T., Stange, P., Taucher, J., Achterberg, E. P., Algueró−Muñiz, M., Horn, H., et al. (2019). The influence of plankton community structure on sinking velocity and remineralization rate of marine aggregates. *Glob. Biogeochem. Cycles* 33, 971–994. doi: 10.1029/2019GB006256

Balch, W. M., Kilpatrick, K., Holligan, P. M., and Cucci, T. (1993). Coccolith production and detachment by *Emiliania Huxleyi* (Prymnesiophyceae). *J. Phycol.* 29, 566–575. doi: 10.1111/j.0022-3646.1993.00566.x

Benner, R., and Amon, R. M. W. (2015). The size-reactivity continuum of major bioelements in the ocean. *Ann. Rev. Mar. Sci.* 7, 185–205. doi: 10.1146/annurev-marine-010213-135126

Bidle, K. D., and Azam, F. (1999). Accelerated dissolution of diatom silica by marine bacterial assemblages. *Nature* 397, 508–512. doi: 10.1038/17351

Blank, G. S., and Sullivan, C. W. (1979). Diatom mineralization of silicic acid. *Arch. Microbiol.* 123, 157–164. doi: 10.1007/BF00446815

Boyd, P. W., Strzepek, R., Fu, F., and Hutchins, D. A. (2010). Environmental control of open-ocean phytoplankton groups: now and in the future. *Limnol. Oceanogr.* 55, 1353–1376. doi: 10.4319/lo.2010.55.3.1353

Boyd, P. W., and Trull, T. W. (2007). Understanding the export of biogenic particles in oceanic waters: is there consensus? *Prog. Oceanogr.* 72, 276–312. doi: 10.1016/j.pocean.2006.10.007

Breuer, G., Lamers, P. P., Martens, D. E., Draaisma, R. B., and Wijffels, R. H. (2012). The impact of nitrogen starvation on the dynamics of triacylglycerol accumulation in nine microalgae strains. *Bioresour. Technol.* 124, 217–226. doi: 10.1016/j.biortech.2012.08.003

Burkhardt, B. G., Watkins-Brandt, K. S., Defforey, D., Paytan, A., and White, A. E. (2014). Remineralization of phytoplankton-derived organic matter by natural populations of heterotrophic bacteria. *Mar. Chem.* 163, 1–9. doi: 10.1016/j.marchem.2014.03.007

Cadée, G. (1985). Macroaggregates of *Emiliana huxleyi* in sediment traps. *Mar. Ecol. Prog. Ser.* 24, 193–196. doi: 10.3354/meps024193

Calvo-Díaz, A., and Morán, X. A. G. (2006). Seasonal dynamics of picoplankton in shelf waters of the southern Bay of Biscay. *Aquat. Microb. Ecol.* 42, 159–174. doi: 10.3354/ame042159

Carlson, C. A., and Hansell, D. A. (2015). "DOM sources, sinks, reactivity, and budgets," in *Biogeochemistry of Marine Dissolved Organic Matter*, 2nd Edn, eds D. A. Hansell and C. A. Carlson (Boston, MA: Academic Press), 65–126. doi: 10.1016/B978-0-12-405940-5.00003-0

Cermeño, P., Dutkiewicz, S., Harris, R. P., Follows, M., Schofield, O., and Falkowski, P. G. (2008). The role of nutricline depth in regulating the ocean carbon cycle. *Proc. Natl. Acad. Sci. U.S.A.* 105, 20344–20349. doi: 10.1073/pnas.0811302106

Cermeño, P., Lee, J. B., Wyman, K., Schofield, O., and Falkowski, P. G. (2011). Competitive dynamics in two species of marine phytoplankton under non-equilibrium conditions. *Mar. Ecol. Prog. Ser.* 429, 19–28. doi: 10.3354/meps09088

Chauton, M. S., Olsen, Y., and Vadstein, O. (2013). Biomass production from the microalga *Phaeodactylum tricornutum*: nutrient stress and chemical composition in exponential fed-batch cultures. *Biomass Bioenergy* 58, 87–94. doi: 10.1016/j.biombioe.2013.10.004

Cramer, W., Kicklighter, D. W., Bondeau, A., Iii, B. M., Churkina, G., Nemry, B., et al. (1999). Comparing global models of terrestrial net primary productivity (NPP): overview and key results. *Glob. Chang. Biol.* 5, 1–15. doi: 10.1046/j.1365-2486.1999.00009.x

Cubillos, J., Wright, S., Nash, G., de Salas, M., Griffiths, B., Tilbrook, B., et al. (2007). Calcification morphotypes of the coccolithophorid *Emiliania huxleyi* in the Southern Ocean: changes in 2001 to 2006 compared to historical data. *Mar. Ecol. Prog. Ser.* 348, 47–54. doi: 10.3354/meps07058

De La Rocha, C. L. (2007). "The biological pump," in *Treatise on Geochemistry*, eds H. D. Holland and K. K. Turekian (Amsterdam: Elsevier), 1–29. doi: 10.1016/B0-08-043751-6/06107-7

De La Rocha, C. L., and Passow, U. (2007). Factors influencing the sinking of POC and the efficiency of the biological carbon pump. *Deep. Res. Part II Top. Stud. Oceanogr.* 54, 639–658. doi: 10.1016/j.dsr2.2007.01.004

del Giorgio, P. A., and Cole, J. J. (1998). Bacterial growth efficiency in natural aquatic systems. *Annu. Rev. Ecol. Syst.* 29, 503–541. doi: 10.1146/annurev.ecolsys.29.1.503

Dunne, J. P., Sarmiento, J. L., and Gnanadesikan, A. (2007). A synthesis of global particle export from the surface ocean and cycling through the ocean interior and on the seafloor. *Glob. Biogeochem. Cycles* 21, 1–16. doi: 10.1029/2006GB002907

Dünweber, M., Swalethorp, R., Kjellerup, S., Nielsen, T. G., Arendt, K. E., Hjorth, M., et al. (2010). Succession and fate of the spring diatom bloom in Disko Bay, western Greenland. *Mar. Ecol. Prog. Ser.* 419, 11–29. doi: 10.3354/meps08813

Durante, G., Basset, A., Stanca, E., and Roselli, L. (2019). Allometric scaling and morphological variation in sinking rate of phytoplankton. *J. Phycol.* 55, 1386–1393. doi: 10.1111/jpy.12916

Egge, J., and Aksnes, D. (1992). Silicate as regulating nutrient in phytoplankton competition. *Mar. Ecol. Prog. Ser.* 83, 281–289. doi: 10.3354/meps083281

Ellegaard, M., Lenau, T., Lundholm, N., Maibohm, C., Friis, S. M. M., Rottwitt, K., et al. (2016). The fascinating diatom frustule—can it play a role for attenuation of UV radiation? *J. Appl. Phycol.* 28, 3295–3306. doi: 10.1007/s10811-016-0893-5

Engel, A., Abramson, L., Szlosek, J., Liu, Z., Stewart, G., Hirschberg, D., et al. (2009). Investigating the effect of ballasting by $CaCO_3$ in *Emiliania huxleyi*, II: decomposition of particulate organic matter. *Deep. Res. Part II Top. Stud. Oceanogr.* 56, 1408–1419. doi: 10.1016/j.dsr2.2008.11.028

Eppley, R. W., and Peterson, B. J. (1979). Particulate organic matter flux and planktonic new production in the deep ocean. *Nature* 282, 677–680. doi: 10.1038/282677a0

Finkel, Z. V., Follows, M. J., Liefer, J. D., Brown, C. M., Benner, I., and Irwin, A. J. (2016). Phylogenetic diversity in the macromolecular composition of microalgae. *PLoS One* 11:e0155977. doi: 10.1371/journal.pone.0155977

Francois, R., Honjo, S., Krishfield, R., and Manganini, S. (2002). Factors controlling the flux of organic carbon to the bathypelagic zone of the ocean. *Glob. Biogeochem. Cycles* 16, 34-1–34-20. doi: 10.1029/2001GB001722

Fritz, J. J. (1999). Carbon fixation and coccolith detachment in the coccolithophore *Emiliania huxleyi* in nitrate-limited cyclostats. *Mar. Biol.* 133, 509–518. doi: 10.1007/s002270050491

Fritz, J. J., and Balch, W. M. (1996). A light-limited continuous culture study of *Emiliania huxleyi*: determination of coccolith detachment and its relevance to cell sinking. *J. Exp. Mar. Bio. Ecol.* 207, 127–147. doi: 10.1016/S0022-0981(96)02633-0

Fujii, M., Murashige, S., Ohnishi, Y., Yuzawa, A., Miyasaka, H., Suzuki, Y., et al. (2002). Decomposition of phytoplankton in seawater. Part I: kinetic analysis of the effect of organic matter concentration. *J. Oceanogr.* 58, 433–438. doi: 10.1023/A:1021296713132

Garnier, J., Beusen, A., Thieu, V., Billen, G., and Bouwman, L. (2010). N:P:Si nutrient export ratios and ecological consequences in coastal seas evaluated by the ICEP approach. *Glob. Biogeochem. Cycles* 24, 1–12. doi: 10.1029/2009GB003583

Giering, S. L. C., Sanders, R., Lampitt, R. S., Anderson, T. R., Tamburini, C., Boutrif, M., et al. (2014). Reconciliation of the carbon budget in the ocean's twilight zone. *Nature* 507, 480–483. doi: 10.1038/nature13123

Goutx, M., Wakeham, S. G., Lee, C., Duflos, M., Guigue, C., Liu, Z., et al. (2007). Composition and degradation of marine particles with different settling velocities in the northwestern Mediterranean Sea. *Limnol. Oceanogr.* 52, 1645–1664. doi: 10.4319/lo.2007.52.4.1645

Grasshoff, K., Kremling, K., and Ehrhardt, M. (eds) (1978). *Methods of Seawater Analysis*, 3rd Edn. Hoboken, NJ: John Wiley & Sons. doi: 10.1016/0304-4203(78)90045-2

Guerrini, F., Cangini, M., Boni, L., Trost, P., and Pistocchi, R. (2000). Metabolic responses of the diatom *Achnanthes brevipes* (Bacillarophyceae) to nutrient limitation. *J. Phycol.* 36, 882–890. doi: 10.1046/j.1529-8817.2000.99070.x

Guidi, L., Stemmann, L., Jackson, G. A., Ibanez, F., Claustre, H., Legendre, L., et al. (2009). Effects of phytoplankton community on production, size, and export of large aggregates: a world-ocean analysis. *Limnol. Oceanogr.* 54, 1951–1963. doi: 10.4319/lo.2009.54.6.1951

Hama, T., Yanagi, K., and Hama, J. (2004). Decrease in molecular weight of photosynthetic products of marine phytoplankton during early diagenesis. *Limnol. Oceanogr.* 49, 471–481. doi: 10.4319/lo.2004.49.2.0471

Hamm, C. E., Merkel, R., Springer, O., Jurkojc, P., Maiert, C., Prechtelt, K., et al. (2003). Architecture and material properties of diatom shells provide effective mechanical protection. *Nature* 421, 841–843. doi: 10.1038/nature 01416

Hansell, D. A. (2013). Recalcitrant dissolved organic carbon fractions. *Ann. Rev. Mar. Sci.* 5, 421–445. doi: 10.1146/annurev-marine-120710-100757

Hansell, D. A., Carlson, C. A., Repeta, D. J., and Schlitzer, R. (2009). Dissolved organic matter in the ocean a controversy stim ulates new insights. *Oceanography* 22, 202–211. doi: 10.5670/oceanog.2009.109

Harvey, H. R., and Macko, S. A. (1997). Kinetics of phytoplankton decay during simulated sedimentation: changes in lipids under oxic and anoxic conditions. *Org. Geochem.* 27, 129–140. doi: 10.1016/S0146-6380(97)00077-6

Harvey, H. R., Tuttle, J. H., and Tyler Bell, J. (1995). Kinetics of phytoplankton decay during simulated sedimentation: changes in biochemical composition and microbial activity under oxic and anoxic conditions. *Geochim. Cosmochim. Acta* 59, 3367–3377. doi: 10.1016/0016-7037(95)00217-N

Henson, S. A., Sanders, R., and Madsen, E. (2012). Global patterns in efficiency of particulate organic carbon export and transfer to the deep ocean. *Glob. Biogeochem. Cycles* 26, 1–14. doi: 10.1029/2011GB004099

Herndl, G. J., and Reinthaler, T. (2013). Microbial control of the dark end of the biological pump. *Nat. Geosci.* 6, 718–724. doi: 10.1038/ngeo1921

Ingalls, A. E., Liu, Z., and Lee, C. (2006). Seasonal trends in the pigment and amino acid compositions of sinking particles in biogenic $CaCO_3$ and SiO_2 dominated regions of the Pacific sector of the Southern Ocean along 170°W. *Deep. Res. Part I Oceanogr. Res. Pap.* 53, 836–859. doi: 10.1016/j.dsr.2006.01.004

Iversen, M. H., and Ploug, H. (2013). Temperature effects on carbon-specific respiration rate and sinking velocity of diatom aggregates – potential implications for deep ocean export processes. *Biogeosciences* 10, 4073–4085. doi: 10.5194/bg-10-4073-2013

Jewell, W. J., and Mccarty, P. L. (1971). Aerobic decomposition of algae. *Environ. Sci. Technol.* 5, 1023–1031. doi: 10.1021/es60057a005

Jiao, N., Herndl, G. J., Hansell, D. A., Benner, R., Kattner, G., Wilhelm, S. W., et al. (2010). Microbial production of recalcitrant dissolved organic matter: long-term carbon storage in the global ocean. *Nat. Rev. Microbiol.* 8, 593–599. doi: 10.1038/nrmicro2386

Jin, X., Gruber, N., Dune, J. P., Sarmiento, J. L., and Armstrong, R. A. (2006). Diagnosing the contributions of phytoplankton functional groups to the production and export of particulate organic carbon, $CaCO_3$, and opal from global nutrient and alkalinity distributions. *Glob. Biogeochem. Cycles* 20, 1–17. doi: 10.1029/2005GB002532

Kirchman, D. L. (2001). "Measuring bacterial biomass production and growth rates from leucine incorporation in natural aquatic environments," in *Methods in Microbiology*, ed. J. H. Paul (St Petersburg, FL: Elsevier), 227–237. doi: 10.1016/S0580-9517(01)30047-8

Kragh, T., Søndergaard, M., and Tranvik, L. (2008). Effect of exposure to sunlight and phosphorus-limitation on bacterial degradation of coloured dissolved organic matter (CDOM) in freshwater. *FEMS Microbiol. Ecol.* 64, 230–239. doi: 10.1111/j.1574-6941.2008.00449.x

Kramer, G., and Herndl, G. (2004). Photo- and bioreactivity of chromophoric dissolved organic matter produced by marine bacterioplankton. *Aquat. Microb. Ecol.* 36, 239–246. doi: 10.3354/ame036239

Kranzler, C. F., Krause, J. W., Brzezinski, M. A., Edwards, B. R., Biggs, W. P., Maniscalco, M., et al. (2019). Silicon limitation facilitates virus infection and mortality of marine diatoms. *Nat. Microbiol.* 4, 1790–1797. doi: 10.1038/s41564-019-0502-x

Kroer, N. (1993). Bacterial growth efficiency on natural dissolved organic matter. *Limnol. Oceanogr.* 38, 1282–1290. doi: 10.4319/lo.1993.38.6.1282

Kuwata, A., Hama, T., and Takahashi, M. (1993). Ecophysiological characterization of two life forms, resting spores and resting cells, of a marine planktonic diatom, *Chaetoceros pseudocurvisetus*, formed under nutrient depletion. *Mar. Ecol. Prog. Ser.* 102, 245–256. doi: 10.3354/meps102245

Kwon, E. Y., Primeau, F., and Sarmiento, J. L. (2009). The impact of remineralization depth on the air–sea carbon balance. *Nat. Geosci.* 2, 630–635. doi: 10.1038/ngeo612

Lam, P. J., and Bishop, J. K. B. (2007). High biomass, low export regimes in the Southern Ocean. *Deep. Res. Part II Top. Stud. Oceanogr.* 54, 601–638. doi: 10.1016/j.dsr2.2007.01.013

Lara, R. J., and Thomas, D. N. (1995). Formation of recalcitrant organic matter: humification dynamics of algal derived dissolved organic carbon and its hydrophobic fractions. *Mar. Chem.* 51, 193–199. doi: 10.1016/0304-4203(95)00066-6

Lennon, J., and Pfaff, L. (2005). Source and supply of terrestrial organic matter affects aquatic microbial metabolism. *Aquat. Microb. Ecol.* 39, 107–119. doi: 10.3354/ame039107

Liefer, J. D., Garg, A., Fyfe, M. H., Irwin, A. J., Benner, I., Brown, C. M., et al. (2019). The macromolecular basis of phytoplankton C:N:P under nitrogen starvation. *Front. Microbiol.* 10:763. doi: 10.3389/fmicb.2019.00763

Madigan, M. T., Martinko, J. M., and Parker, J. (1997). *Brock Biology of Microorganisms*. Upper Saddle River, NJ: Prentice hall.

Marañón, E., Cermeño, P., López-Sandoval, D. C., Rodríguez-Ramos, T., Sobrino, C., Huete-Ortega, M., et al. (2013). Unimodal size scaling of phytoplankton growth and the size dependence of nutrient uptake and use. *Ecol. Lett.* 16, 371–379. doi: 10.1111/ele.12052

Martin, J. H., Knauer, G. A., Karl, D. M., and Broenkow, W. W. (1987). VERTEX: carbon cycling in the northeast Pacific. *Deep Sea Res. Part A. Oceanogr. Res. Pap.* 34, 267–285. doi: 10.1016/0198-0149(87)90086-0

Martin, P., Lampitt, R. S., Jane Perry, M., Sanders, R., Lee, C., and D'Asaro, E. (2011). Export and mesopelagic particle flux during a North Atlantic spring diatom bloom. *Deep. Res. Part I Oceanogr. Res. Pap.* 58, 338–349. doi: 10.1016/j.dsr.2011.01.006

Menden-Deuer, S., and Lessard, E. J. (2000). Carbon to volume relationships for dinoflagellates, diatoms, and other protist plankton. *Limnol. Oceanogr.* 45, 569–579. doi: 10.4319/lo.2000.45.3.0569

Merico, A., Tyrrell, T., Brown, C. W., Groom, S. B., and Miller, P. I. (2003). Analysis of satellite imagery for *Emiliania huxleyi* blooms in the Bering Sea before 1997. *Geophys. Res. Lett.* 30:1337. doi: 10.1029/2002GL016648

Moriceau, B., Goutx, M., Guigue, C., Lee, C., Armstrong, R., Duflos, M., et al. (2009). Si-C interactions during degradation of the diatom *Skeletonema marinoi*. *Deep. Res. Part II Top. Stud. Oceanogr.* 56, 1381–1395. doi: 10.1016/j.dsr2.2008.11.026

Nelson, D. M., Tréguer, P., Brzezinski, M. A., Leynaert, A., and Quéguiner, B. (1995). Production and dissolution of biogenic silica in the ocean: revised global estimates, comparison with regional data and relationship to biogenic sedimentation. *Glob. Biogeochem. Cycles* 9, 359–372. doi: 10.1029/95GB01070

Norland, S. (1993). "The relationship between biomass and volume of bacteria," in *Handbook of Methods in Aquatic Microbial Ecology*, eds P. F. Kemp, J. J. Cole, B. F. Sherr, and E. B. Sherr (Boca Raton, FL: Lewis Publishers), 303–307.

Oku, O., and Kamatani, A. (1997). Resting spore formation of the marine planktonic diatom *Chaetoceros anastomosans* induced by high salinity and nitrogen depletion. *Mar. Biol.* 127, 515–520. doi: 10.1007/s002270050040

Omand, M. M., D'Asaro, E. A., Lee, C. M., Perry, M. J., Briggs, N., Cetinić, I., et al. (2015). Eddy-driven subduction exports particulate organic carbon from the spring bloom. *Science* 348, 222–225. doi: 10.1126/science.1260062

Padisák, J., Soróczki-Pintér, É, and Rezner, Z. (2003). "Sinking properties of some phytoplankton shapes and the relation of form resistance to morphological diversity of plankton — an experimental study," in *Aquatic Biodiversity*, ed. K. Martens (Dordrecht: Springer), 243–257. doi: 10.1007/978-94-007-1084-9_18

Panagiotopoulos, C., Sempéré, R., Obernosterer, I., Striby, L., Goutx, M., Van Wambeke, F., et al. (2002). Bacterial degradation of large particles in the southern Indian Ocean using in vitro incubation experiments. *Org. Geochem.* 33, 985–1000. doi: 10.1016/S0146-6380(02)00057-8

Passow, U., French, M. A., and Robert, M. (2011). Biological controls on dissolution of diatom frustules during their descent to the deep ocean: lessons learned from controlled laboratory experiments. *Deep. Res. Part I Oceanogr. Res. Pap.* 58, 1147–1157. doi: 10.1016/j.dsr.2011.09.001

Pinhassi, J., Gómez-Consarnau, L., Alonso-Sáez, L., Sala, M., Vidal, M., Pedrós-Alió, C., et al. (2006). Seasonal changes in bacterioplankton nutrient limitation and their effects on bacterial community composition in the NW Mediterranean Sea. *Aquat. Microb. Ecol.* 44, 241–252. doi: 10.3354/ame044241

Pomeroy, L. R., and Deibel, D. (1986). Temperature regulation of bacterial activity during the spring bloom in Newfoundland coastal waters. *Science* 233, 359–361. doi: 10.1126/science.233.4761.359

Rembauville, M., Manno, C., Tarling, G. A., Blain, S., and Salter, I. (2016). Strong contribution of diatom resting spores to deep-sea carbon transfer in naturally

iron-fertilized waters downstream of South Georgia. *Deep. Res. Part I Oceanogr. Res. Pap.* 115, 22–35. doi: 10.1016/j.dsr.2016.05.002

Rost, B., and Riebesell, U. (2004). "Coccolithophores and the biological pump: responses to environmental changes," in *Coccolithophores*, eds H. R. Thierstein and J. R. Young (Berlin: Springer), 99–125. doi: 10.1007/978-3-662-06278-4_5

Rynearson, T. A., Richardson, K., Lampitt, R. S., Sieracki, M. E., Poulton, A. J., Lyngsgaard, M. M., et al. (2013). Major contribution of diatom resting spores to vertical flux in the sub-polar North Atlantic. *Deep. Res. Part I Oceanogr. Res. Pap.* 82, 60–71. doi: 10.1016/j.dsr.2013.07.013

Sala, M. M., Peters, F., Gasol, J. M., Pedrós-Alió, C., Marrasé, C., and Vaqué, D. (2002). Seasonal and spatial variations in the nutrient limitation of bacterioplankton growth in the northwestern Mediterranean. *Aquat. Microb. Ecol.* 27, 47–56. doi: 10.3354/ame027047

Salter, I., Kemp, A. E. S., Moore, C. M., Lampitt, R. S., Wolff, G. A., and Holtvoeth, J. (2012). Diatom resting spore ecology drives enhanced carbon export from a naturally iron-fertilized bloom in the Southern Ocean. *Glob. Biogeochem. Cycles* 26:GB1014. doi: 10.1029/2010GB003977

Schmittner, A., Oschlies, A., Matthews, H. D., and Galbraith, E. D. (2008). Future changes in climate, ocean circulation, ecosystems, and biogeochemical cycling simulated for a business-as-usual CO_2 emission scenario until year 4000 AD. *Glob. Biogeochem. Cycles* 22:GB1013. doi: 10.1029/2007GB002953

Sempéré, R., Yoro, S. C., Van Wambeke, F., and Charrière, B. (2000). Microbial decomposition of large organic particles in the northwestern Mediterranean Sea: an experimental approach. *Mar. Ecol. Prog. Ser.* 198, 61–72. doi: 10.3354/meps198061

Siegel, D. A., Buesseler, K. O., Doney, S. C., Sailley, S. F., Behrenfeld, M. J., and Boyd, P. W. (2014). Global assessment of ocean carbon export by combining satellite observations and food-web models. *Glob. Biogeochem. Cycles* 28, 181–196. doi: 10.1002/2013GB004743

Smith, D. C., Simon, M., Alldredge, A. L., and Azam, F. (1992). Intense hydrolytic enzyme activity on marine aggregates and implications for rapid particle dissolution. *Nature* 359, 139–142. doi: 10.1038/359139a0

Steinberg, D. K., and Landry, M. R. (2017). Zooplankton and the ocean carbon cycle. *Ann. Rev. Mar. Sci.* 9, 413–444. doi: 10.1146/annurev-marine-010814-015924

Stone, R. (2010). The invisible hand behind a vast carbon reservoir. *Science* 328, 1476–1477. doi: 10.1126/science.328.5985.1476

Strom, S. L., Benner, R., Ziegler, S., and Dagg, M. J. (1997). Planktonic grazers are a potentially important source of marine dissolved organic carbon. *Limnol. Oceanogr.* 42, 1364–1374. doi: 10.4319/lo.1997.42.6.1364

Suroy, M., Panagiotopoulos, C., Boutorh, J., Goutx, M., and Moriceau, B. (2015). Degradation of diatom carbohydrates: a case study with N- and Si-stressed *Thalassiosira weissflogii*. *J. Exp. Mar. Bio. Ecol.* 470, 1–11. doi: 10.1016/j.jembe.2015.04.018

Thingstad, T. F., Zweifel, U. L., and Rassoulzadegan, F. (1998). P limitation of heterotrophic bacteria and phytoplankton in the northwest Mediterranean. *Limnol. Oceanogr.* 43, 88–94. doi: 10.4319/lo.1998.43.1.0088

Thomsen, L., Aguzzi, J., Costa, C., De Leo, F., Ogston, A., and Purser, A. (2017). The oceanic biological pump: rapid carbon transfer to depth at continental margins during winter. *Sci. Rep.* 7:10763. doi: 10.1038/s41598-017-11075-6

Tréguer, P., Nelson, D. M., Van Bennekom, A. J., Demaster, D. J., Leynaert, A., and Quéguiner, B. (1995). The silica balance in the world ocean: a reestimate. *Science* 268, 375–379. doi: 10.1126/science.268.5209.375

Turner, R. E., Qureshi, N., Rabalais, N. N., Dortch, Q., Justic, D., Shaw, R. F., et al. (1998). Fluctuating silicate:nitrate ratios and coastal plankton food webs. *Proc. Natl. Acad. Sci. U.S.A.* 95, 13048–13051. doi: 10.1073/pnas.95.22.13048

Turner, R. E., Rabalais, N. N., Justic', D., and Dortch, Q. (2003). Global patterns of dissolved N, P and Si in large rivers. *Biogeochemistry* 64, 297–317. doi: 10.1023/A:1024960007569

Utermöhl, H. (1958). Zur Vervollkommnung der quantitativen Phytoplankton-Methodik. *SIL Commun. 1953-1996* 9, 1–38. doi: 10.1080/05384680.1958.11904091

Van Wambeke, F., Christaki, U., Giannakourou, A., Moutin, T., and Souvemerzoglou, K. (2002). Longitudinal and vertical trends of bacterial limitation by phosphorus and carbon in the Mediterranean Sea. *Microb. Ecol.* 43, 119–133. doi: 10.1007/s00248-001-0038-4

Yamamuro, M., and Kayanne, H. (1995). Rapid direct determination of organic carbon and nitrogen in carbonate-bearing sediments with a Yanaco MT-5 CHN analyzer. *Limnol. Oceanogr.* 40, 1001–1005. doi: 10.4319/lo.1995.40.5.1001

Yang, Z.-K., Niu, Y.-F., Ma, Y.-H., Xue, J., Zhang, M.-H., Yang, W.-D., et al. (2013). Molecular and cellular mechanisms of neutral lipid accumulation in diatom following nitrogen deprivation. *Biotechnol. Biofuels* 6:67. doi: 10.1186/1754-6834-6-67

Yentsch, C. S., and Menzel, D. W. (1963). A method for the determination of phytoplankton chlorophyll and phaeophytin by fluorescence. *Deep Sea Res. Oceanogr. Abstr.* 10, 221–231. doi: 10.1016/0011-7471(63)90358-9

Conflict of Interest: The authors declare that the research was conducted in the absence of any commercial or financial relationships that could be construed as a potential conflict of interest.